Application Note
Mar 2021
AN-850-0109

Detection of Pressure-Induced Aggregation Using Microfluidic Modulation Spectroscopy (MMS)

- [x] Research
- [x] Discovery
- [ ] Formulation and Development
- [x] Quality Control
- [ ] Manufacturing

- [x] Aggregation
- [ ] Quantitation
- [x] Stability
- [x] Structure
- [x] Similarity

Introduction

Protein aggregation is a recognized signal of instability and can lead to the loss of protein function. It is therefore crucial to detect protein aggregation early in the drug development process to inform further drug development decisions. Pressure, a stressor used for generating aggregates by impacting noncovalent interactions without the need to change temperature or solvents[1], was employed to create aggregated protein for this spiked study.

The RedShiftBio AQS$^{3®}$pro system, powered by Microfluidic Modulation Spectroscopy (MMS), enables the early detection of instability by measuring minute changes in antiparallel beta-sheet composition, an indicator of irreversible aggregation.[2] The AQS^{3}pro utilizes a high-power quantum cascade laser (QCL) to generate unrivaled sensitivity in secondary structure determination over a wide concentration range. The ability to see change in antiparallel beta sheet composition through stability monitoring at selected wavenumbers by MMS creates an advantage of correlating drug development conditions to potential detrimental effects on protein function at all stages of drug development.

Methods

Soluble aggregates of Human gamma-globulin (IgG, Sigma Cat #G-4386) were generated using a Pressure BioSciences Barocycler®2320EXT. The IgG was prepared in PBS with 10% n-propanol and divided into two aliquots: one aliquot was stressed at 54.5 kpsi in a Pressure BioSciences Barocycler for 30 minutes at room temperature, and a second control aliquot was left untreated. Both samples were incubated overnight at room temperature.

The pressure-treated IgG sample was centrifuged at 9000 g for 15 minutes to remove large insoluble aggregates. The supernatant was collected and its concentration was measured as 7 mg/mL by Bradford assay. The untreated control was diluted to 7 mg/mL to match the treated sample concentration and confirmed by Bradford Assay.

To prepare the samples for MMS analysis, the pressure-treated sample containing the soluble aggregates was spiked into the untreated control (v/v) to generate a series of 11 total samples with different percentages of treated IgG spike ranging from 0% to 100% (Table 1). Each sample was analyzed in duplicate by MMS using the AQS^{3}pro system and spectral data was processed using the Data Analysis processing feature of the AQS^{3}delta software package.

Sample Number	% Aggregated IgG Spike (v/v)
1	0 (untreated control)
2	0.05
3	0.1
4	0.5
5	1
6	5
7	10
8	25
9	50
10	75
11	100 (treated IgG)

Table 1: Percent Aggregated IgG Spike Series

Application Note
Mar 2021

Results

I. Absolute Absorbance and Second Derivative Spectra: The averaged Absolute Absorbance spectra of the 11 samples are shown as overlaid traces in Figure 1A (left). The absolute absorbance was calculated and plotted after concentration normalization and buffer subtraction. To emphasize the differences in these two regions, second derivative plots from spectra for all aggregated spike samples were overlaid as shown in Figure 1B (right).

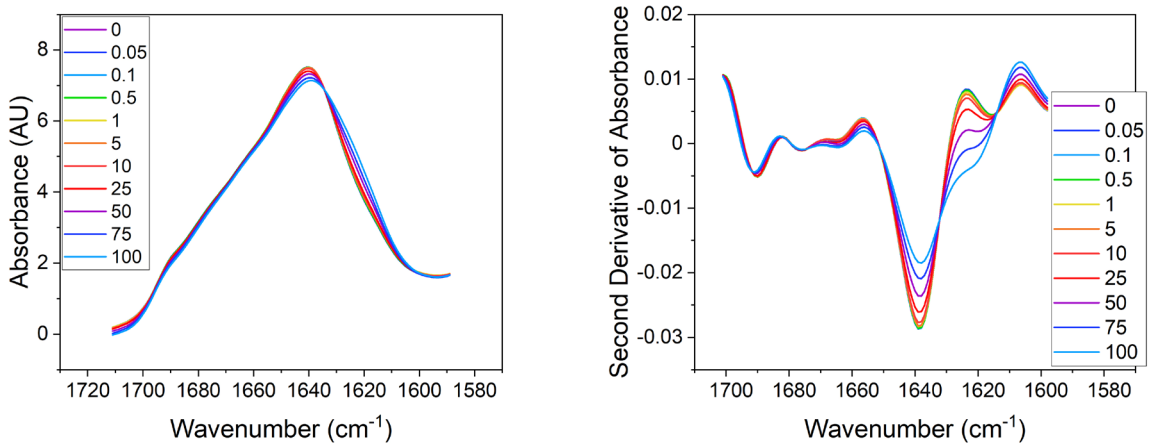

Figure 1: A) Absolute Absorbance spectra of Aggregated IgG Spike Series (left)
B) Second Derivative of the Absolute Absorbance plots for Aggregated IgG Spike Series (right)

The Second Derivative plot highlights the significant changes present in the spectral regions of 1624 and, 1640cm^{-1} that can be seen only subtly in the Absolute Absorbance spectral plot. This data shows, among other noticeable changes in several regions of the spectra, that as the percent of spiked aggregated IgG was increased, the peak at 1640 cm^{-1} (parallel beta-sheet region) decreased while the signal around 1620 cm^{-1} (antiparallel beta sheet) increased.

II. Area of Overlap and Similarity: The Area of Overlap results were derived from the baseline-subtracted second derivative of the absolute absorbance spectra and overlaid (spectra not shown). These results are listed in Table 2 and were reported as percent similarity between samples using the untreated 0% aggregated spike sample as the control.

Sample (% Aggregated Spike)	% Similarity (Area of Overlap)*
0*	100
0.05	99.6
0.1	99.5
0.5	99.5
1	99.4
5	99.0
10	98.0
25	95.3
50	91.2
75	87.5
100	83.9

Table 2: Percent Similarity Results for Aggregated IgG Spike Samples

Application Note
Mar 2021

Results, continued

Figure 2 shows a graph of the percent similarity calculated from the Area of Overlap and it demonstrates that as the percent of aggregated IgG spike increased, the similarity of samples compared to the untreated control decreased linearly as indicated by an R^2 value of nearly 1. This confirms that as more spiked aggregate was added to the series of samples, there was a greater difference and lesser similarity measured between the spiked samples and the untreated control across the whole series.

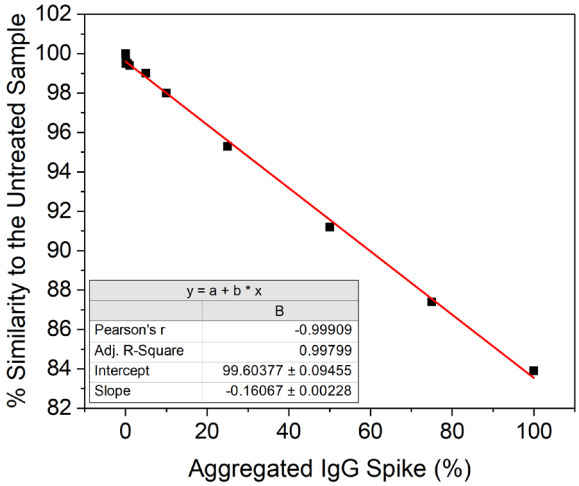

Figure 2: Percent Similarity vs Percent Aggregated IgG Spike Relative to 0% Aggregated Control

III. Delta and Stability: The Delta plot shown in Figure 3A (left) represents the differences between the second derivative of each sample and the control. It is clear from this plot that the spectral regions of 1640 and 1624 cm^{-1} show the most change. The Stability plot shown in Figure 3B (right) tracked changes observed at specific wavenumbers of 1624, 1640, 1656, and 1697 cm^{-1} relating to antiparallel beta-sheet, parallel beta-sheet, alpha-helix, and another antiparallel beta-sheet region, respectively[3] calculated from the Delta Plot. This shows that the region of 1624 cm^{-1} associated with antiparallel beta-sheet content significantly increased and the region of 1640 cm^{-1} associated with parallel beta-sheet content significantly decreased.

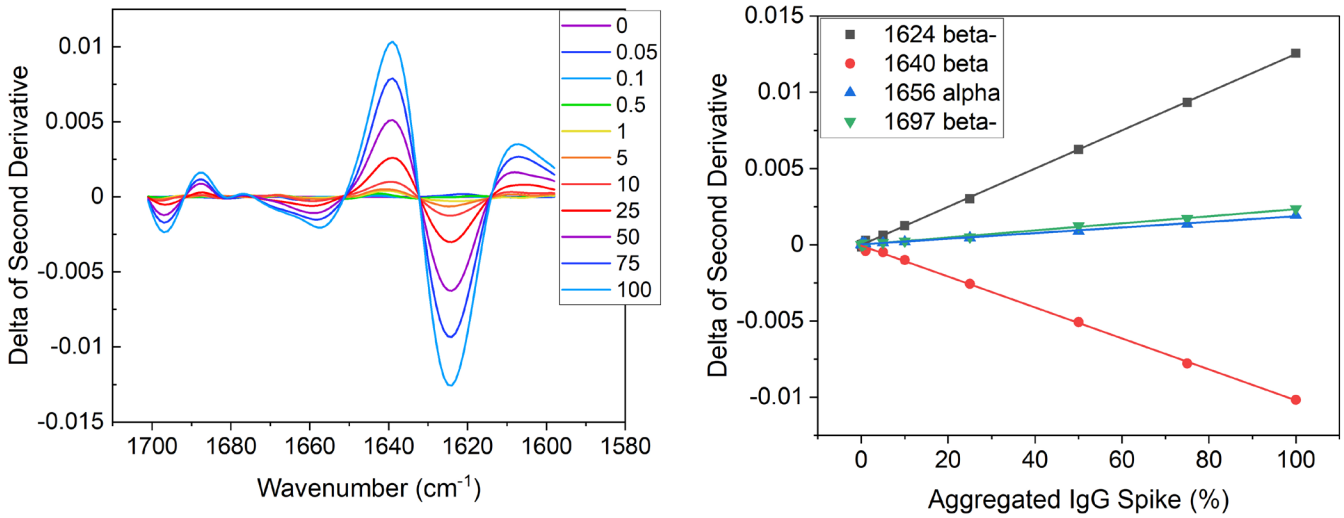

Figure 3: A) Delta of Second Derivative Plot for Aggregated IgG Spike Series (left)
B) Stability Plot for Delta of Second Derivative: 1624, 1640, 1656, and 1697 cm^{-1} (right)

Application Note
Mar 2021

Results, continued

The 1624 cm^{-1} signal correlating to antiparallel beta-sheet content was isolated and plotted versus percent aggregated spike composition to focus on the structural changes associated with aggregation (FIgure 4). The plot shows that the calculated amount of aggregated protein is linearly proportional to percent aggregated spike composition with an R^2 value close to 1.

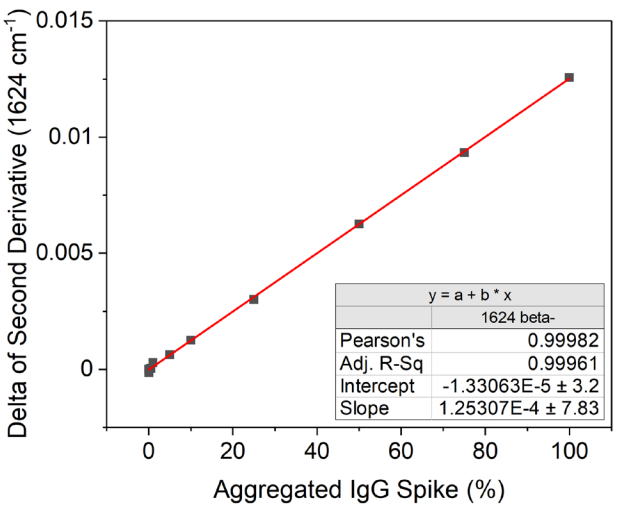

Figure 4: Linear Regression of 1624 cm^{-1} Antiparallel Beta Signal vs Percent Aggregated Spike Series

IV. Weighted Spectral Difference: Another metric used to monitor change in sample secondary structure for this aggregtation study was Weighted Spectral Difference (WSD). This algorithm measures full-spectrum differences from the second derivative plots between the aggregated spike samples relative to the untreated 0% aggregrated spike sample and assigns a greater weighted value to the regions of higher absorbance so that variations in the noise do not interfere with structural changes in more important spectral regions.

For the WSD results, the samples that reported values closer to zero indicate greater similarity to the untreated control sample. Conversely, the larger the WSD value calculated, the more the samples differ.[4,5] Figure 5 shows the WSD results for the increasing aggregated spike samples vs the 0% aggregated control, and it confirms a linear correlation as indicated by the R^2 value close to 1.

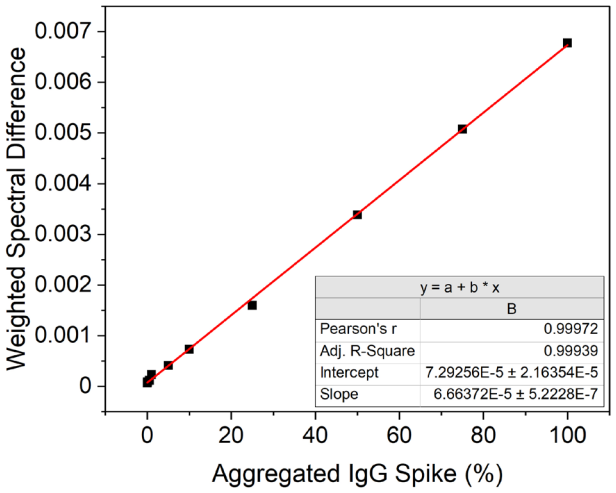

Figure 5: Weighted Spectral Difference of IgG Spike Series vs Untreated IgG 0% Control

V. HOS: Higher Order Structure (HOS) analysis for five structures was calculated and is shown as the HOS bar graph in Figure 6. This data confirms that increasing the percent aggregated spike in the samples resulted in a decrease in overall parallel beta-sheet content (labeled beta) and a consequential increase in overall antiparallel beta-sheet content (labeled beta -). The analysis shows that there are also changes in turn, alpha, and unordered structures as the amount of aggregated spiked protein was increased.

Application Note
Mar 2021

Results, continued

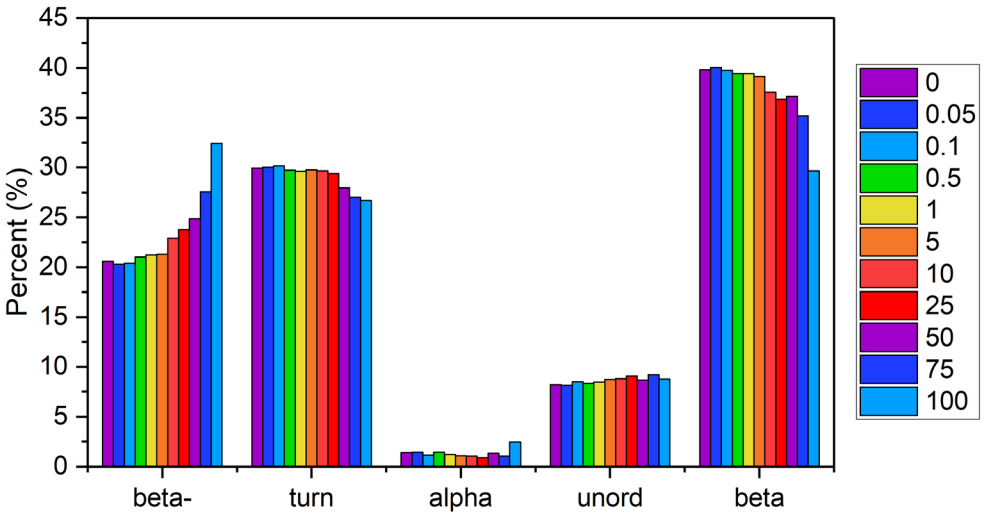

Figure 6: HOS Bar Graph Showing Changes in Antiparallel Beta-sheet (beta-) and Parallel Beta-sheet (beta)

Conclusions

The ability to detect protein aggregation is important at all stages of drug development. Early detection of aggregation is most desirable to inform development decisions since aggregation can negatively affect the functionality of a protein. The Pressure BioSciences Barocycler®2320EXT was successfully used to create stable IgG aggregates for an increasing spiked aggregate series of samples that was analyzed by MMS. The samples were compared using AQS^{3}delta software and the Stability, Similarity, and WSD were calculated relative to an untreated 0% aggregrated spike control. The results consistently showed a strong linear correlation between increasing amounts of percent aggregation and increasing amounts of measured antiparallel beta-sheet content, as the formation of antiparallel beta-sheets is one of the hallmarks of the aggregation process[2,6]. This study demonstrates that the AQS^{3}pro, powered by MMS technology, can successfully be used to detect changes in aggregation at different drug development stages including formulation screening, manufacturing, and storage.

Primary Author: V. Ivancic, Ph.D.

References

1. Daniel, I.; Oger, P.; and Winter, R., Origins of life and biochemistry under higher-pressure conditions. Chemical Society Reviews 2006, 35 (1), 858-875.
2. Wang, W.; and Roberts, C.J., (2010) 'Protein aggregation pathways, kinetics, and thermodynamics' (Li, Y. and Roberts, C.J.) and 'Case studies involving protein aggreation' (Rajan, R.S.; Li, T.; and Arakawa, T.) In Aggregation of Therapeutic Proteins, John Wiley & Sons, 63-102 and 367-396.
3. Dong, A.; Huang, P.; Caughey, W. S., Protein secondary structures in water from second-derivative amide I infrared spectra. Biochemistry 1990, 29 (13), 3303-3308.
4. Dinh, N. N.; Winn, B. C.; Arthur, K. K.; Gabrielson, J. P. Quantitative Spectral Comparison by Weighted Spectral Difference for Protein Higher Order Structure Confirmation. Analytical Biochemistry 2014, 464, 60–62.
5. Kendrick, B.S.; Gabrielson, J.P.; Solsberg, C.W.; Ma, E.; and Wang, L., Determining spectroscopic quantitation limits for misfolded structures. Journal of Pharmaceutical Sciences 2020, 109 (1), 933-936.
6. Chiti, F.; and Dobson, C.M., Protein misfolding, amyloid formation, and human disease: A summary of progress over the last decade. Annu. Rev. Biochem 2017, 86:27-68.

Contributor

Pressure BioSciences, Inc.
14 Norfolk Avenue
South Easton, MA 02375

Contact

RedShift BioAnalytics, Inc
131 Middlesex Turnpike | Burlington, MA | 01803
T: 781.345.7300 | F: 781.345.7301 | E: info@redshiftbio.com